Journal of Pharmaceutical Sciences 106 (2017) 3171-3176

Contents lists available at ScienceDirect

Journal of Pharmaceutical Sciences

journal homepage: www.jpharmsci.org

Note

Pharmaceutical Film Coating Catalog for Spectral Domain Optical Coherence Tomography

Hungyen Lin [1,*], Yue Dong [2], Daniel Markl [3], Zijian Zhang [2], Yaochun Shen [2], J. Axel Zeitler [3]

[1] Department of Engineering, Lancaster University, Lancaster LA1 4YW, UK
[2] Department of Electrical Engineering and Electronics, University of Liverpool, Liverpool L69 3GJ, UK
[3] Department of Chemical Engineering and Biotechnology, University of Cambridge, Cambridge CB2 0AS, UK

ARTICLE INFO

Article history:
Received 22 February 2017
Revised 19 May 2017
Accepted 24 May 2017
Available online 15 June 2017

Keywords:
optical coherence tomography
pharmaceutical film coating
coating thickness

ABSTRACT

Optical coherence tomography (OCT) has recently been demonstrated to measure the film coating thickness of pharmaceutical tablets and pellets directly. The results enable the analysis of inter- and intra-tablet coating variability at an off-line and in-line setting. To date, only a few coating formulations have been tried and there is very little information on the applicability of OCT to other coatings. As it is well documented that optical methods including OCT are prone to scattering leading to limited penetration, some pharmaceutical coatings may not be measurable altogether. This study presents OCT measurements of 22 different common coatings for the assessment of OCT applicability.

Introduction

Film coatings serve the very purpose of achieving color uniformity, light protection, and taste masking. Coatings are additionally used to modify the drug release or to incorporate an active pharmaceutical ingredient in the formulation. Coating quality can be studied either by numerical modeling[1] or by the aid of process analyzers. Various process analytical technology approaches have been demonstrated for characterizing pharmaceutical coating, which include near-infrared and Raman spectroscopy,[2-4] nuclear magnetic resonance imaging,[5] terahertz pulsed imaging (TPI),[6-8] and optical coherence tomography (OCT).[9-15] Among these methods, TPI and OCT are attractive because they offer a direct, calibration-free coating thickness measurement, where the only unknown is the coating refractive index that can be obtained as a one-off measurement with terahertz time-domain spectroscopy and spectroscopic ellipsometry, respectively. Comparing the two, TPI has limited resolution (i.e., a lateral spatial of 200 μm and axial [depth] resolution of 2 μm for coating thickness greater than 30-40 μm) and requires relatively long measurement times (in the range of 8 ms). OCT, in contrast, can achieve sub-μm resolutions for coating thickness greater than 10 μm and exploits an μs acquisition time leading to information on both inter-tablet and intra-tablet coating variation. Specifically, OCT has been demonstrated in an off-line[9-11] and in-line setting for characterizing pellets[12,13] and tablets.[14,15] However, OCT has limited penetration depth than TPI, and in some cases fails to image through coatings altogether. This limitation originates from a similar refractive index between the tablet core and coating leading to weaker reflections, and/or pronounced scattering encountered as the optical beam penetrates into the sample, resulting in substantial signal attenuation. These effects ultimately limit the resolvable coating thickness. There is currently very little information available in the literature on what coating materials can or cannot be imaged using OCT technology. This study therefore aims to examine the transparency of a range of coating formulations for OCT measurement at 840 nm.

Materials and Methods

Tablet Production

The samples used in the present work comprise 22 randomly selected tablets from 22 different batches where a different coating formulation was used for each of the batches. The coating product name, the corresponding alias, and photographs of the tablets are shown in Table 1. Coating materials were applied to

This article contains supplementary material available from the authors by request or via the Internet at http://dx.doi.org/10.1016/j.xphs.2017.05.032.

* *Correspondence to:* Hungyen Lin (Telephone: +44 1524 593013; Fax: +44 1524 381707).
E-mail address: h.lin2@lancaster.ac.uk (H. Lin).

http://dx.doi.org/10.1016/j.xphs.2017.05.032

bi-convex-shaped tablet cores that contained 50% lactose monohydrate and 50% microcrystalline cellulose. Film coating was performed with a 15″ fully perforated Labcoat IIX (O'Hara Technologies Inc., Richmond Hill, ON) equipped with one spray nozzle (Model 970; Düsen-Schlick GmbH, Untersiemau, Germany). The coating pan has a diameter of 380 mm and a full volume of 4.5 L enabling a batch size of 500 g. Average thickness, diameter, and weight of the tablet cores ($n = 6$) were 4.079 ± 0.018 mm, 10.069 ± 0.005 mm, and 321 ± 3 mg, respectively. For measurement comparisons, one side of the tablets was marked by a scratch mark to serve as a datum. Film coating thickness was estimated by measuring the physical dimensions of coated tablets with a micrometer gauge and subtracting it away from the average core thickness, assuming no dimensional changes to the cores in the coating process.

Spectral Domain Optical Coherence Tomographic Measurements

An in-house fiber-based spectral domain OCT system[16] was developed for B-scan measurements of the coated tablets. As shown in Figure 1, a superluminescent diode (EXALOS AG, Schlieren, Switzerland) centered at a wavelength of 840 nm with a full width at half maximum bandwidth of 55 nm was used as the light source. The light source provided a theoretical axial resolution of 5.7 μm in air. The collimated light beam was first coupled into the input port of a 2 × 2 wideband single mode fiber coupler using a collimator. The light beam was subsequently split (50:50) into a reference and a probe beam. The reference beam was collimated by an adjustable collimator (CFC-2X-B; Thorlabs Inc., Newton, NJ) and reflected by a reference mirror. The probe beam was focused onto the tablet surface by another identical adjustable collimator. The focal length was 7 mm, which lead to a lateral resolution of 20 μm and a depth of field of 734 μm. The backscattered probe beam interfered with the reflected reference beam at the output port of the fiber coupler. The interferogram was collected by a high resolution spectrometer (Wasatch Photonics Inc., Logan, UT) consisting of 2048 pixels linear array CCD camera. In order to obtain a B-scan (cross-sectional image) across the tablet surface, a translation stage was used to move the tablet sample at a velocity of 1 mm/s by a motorized stage. The spectrometer was set to acquire a spectrum every 6 ms with an exposure time of 90 μs. In total, 1000 A-scans, which covered a length of 6 mm with an equivalent step size of 6 μm, were acquired for each tablet to generate a B-scan. The measured optical spot size on the tablet surface was approximately 20 μm. Measurements were performed perpendicular to the overall tablet surface plane at the tablet center as opposed to being perpendicular to the tablets' curved surface.[6,7] As such, only the coating thickness at the tablet central region can be accurately measured unless the tablet curvature is accounted for.[17] The coating thickness is proportional to the separation between adjacent reflection peaks in an A-scan and is determined using $d = \Delta tc/(2n)$, where d is the coating thickness, c the speed of light, Δt the peak separation, and n the coating refractive index.

Table 1
Images of the Tablets Coated With the Respective Coating Product and the Corresponding Alias

Coating	Product ID		Product ID		Product ID	
Coating 1	03F190003 (opadry)		Coating 9	03F220071	Coating 17	114F210058
Coating 2	20A29015 (opadry)		Coating 10	33G200004	Coating 18	114F250049
Coating 3	31F29070 (opadry II)		Coating 11	03B205020 (opadry)	Coating 19	200F220052
Coating 4	45F29058 (opadry II)		Coating 12	03F205017	Coating 20	493Z240008
Coating 5	02A240002 (opadry)		Coating 13	85F205105	Coating 21	TC-117-205006
Coating 6	02B220014		Coating 14	85G200008	Coating 22	TC-116-205001
Coating 7	85F190000 (opadry II)		Coating 15	88A210007 (opadry amb II)		
Coating 8	70W29079 (opadry ns-g)		Coating 16	112A210011		

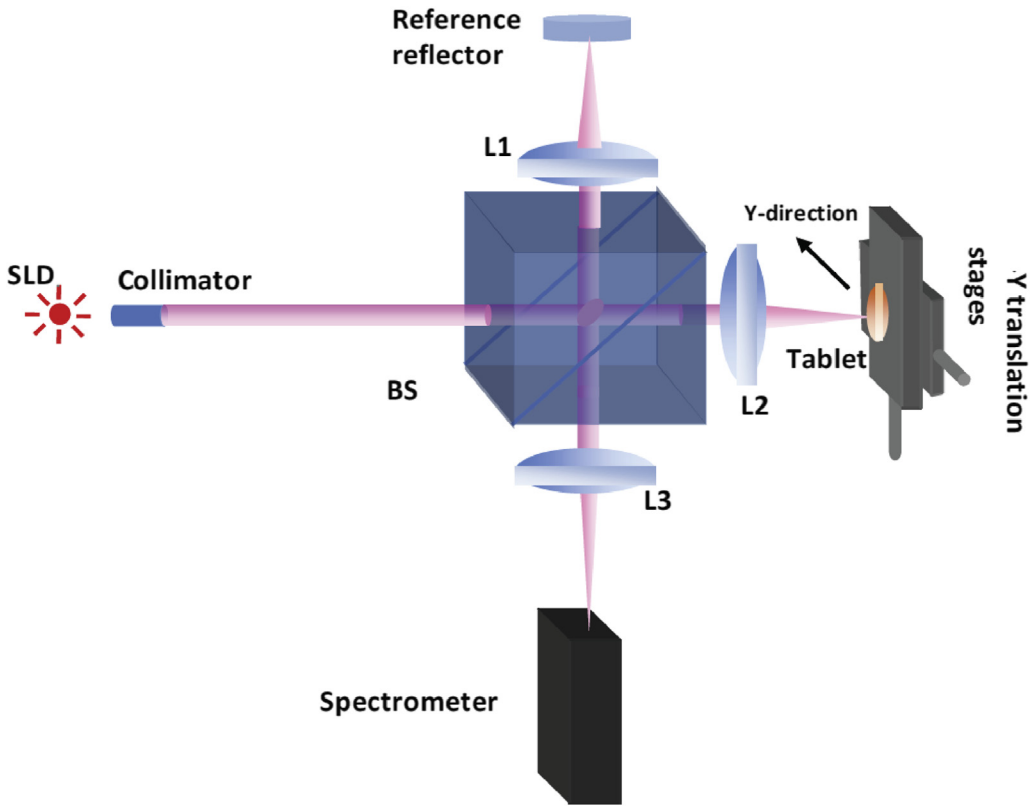

Figure 1. Schematic of an in-house spectral domain OCT system with a tablet placed in the perforated coating pan. C1 and C2, adjustable collimators; L1, L2, and L3, lens; BS, beam-splitter; SLD, superluminescent diode.

X-Ray Computed Microtomography

X-ray computed microtomography (XμCT) measurement was performed on a SkyScan 1172 (control software: Skyscan1172 XμCT Control Program v1.5; Bruker, Kontich, Belgium). Reconstruction was performed using the program NRecon (Bruker, v1.6.9.8) on a single PC using graphical processing unit accelerated reconstruction (Windows 7 64-bit workstation, 2 Intel Xeon X5647 with 4 cores each, 48 GB RAM, NVIDIA Quadro 4000 with 256 cores) yielding 3-dimensional data with an isotropic voxel size of 0.95 μm. The data acquisition time was 4 h and the image reconstruction took 0.5 h size for 433 slices of 1116 × 1116 pixels.

Results and Discussions

Figure 2 shows the acquired B-scans of the 22 coated tablets. Evidently, the coating-core interface for coatings 1, 2, 7, 8, 13, and 18 can be visibly observed. The level of contrast between the air-coating and coating-core interface in coatings 1, 4, and 13 may be enhanced with signal denoising.[16] It should be noted that in order to quantify the absolute coating thickness, a clear observation of the coating-core interface and knowledge of the coating refractive index is required.[16,17] As refractive index remains unknown in this study, coating thickness is not determined but instead, estimated using a micrometer gauge. As a quick check, we measured coating 9 using XμCT, sub-volume shown in Supplementary Figure S1, that yielded a thickness of 51.0 ± 6.2 μm ($n = 10$) in agreement with the estimated thickness of 59 ± 10 μm. No thickness information could be derived with OCT in this instance due to an absence of the coating-core interface. Closer inspection of Supplementary Figure S1 also shows that some of the coating has fused into the tablet core,[18,19] which would have caused a gradual refractive index change leading to low contrast in OCT measurement. To better isolate the causes behind OCT opaqueness at 840 nm, the coating compositions for the respective coatings are listed in Table 2. In coating compositions without pigments or colorants, generally the coating-core interface in B-scans is visible. Coatings 1 and 3, however, are notable exceptions because of the additional lactose and polydextrose, which may have increased scattering and reduced the refractive index contrast between the core and coating as the core also contained 50% lactose monohydrate. This would then reduce the reflected signal intensity from the coating-core interface, resulting in no clear observation of the coating-core interface on the B-scan. Assuming negligible optical absorption in the polymer binder,[20] for compositions containing pigments, in particular, titanium dioxide, the coating-core interface is not visible at all. This is due to the pigment particle size and a relatively high value of the effective refractive index that in turn increases reflection at the air-coating interface, meaning that only a fraction of incidence beam can actually penetrate into the coating.[20] As the remaining beam travels into the coating, more scattering is encountered leading to a further signal reduction for measurement. The scattering effect for yellow iron oxide compared to titanium dioxide is generally weaker at near-infrared wavelengths.[21] Despite this, coating 9 is still opaque to OCT because of the gradual refractive index change encountered because the coating dispersion has diffused into the core material.[18,19] On the contrary, 3% weight gain red coating (coating 18) is transparent to OCT largely due to a comparatively larger difference between the coating and core refractive index in spite of the increased air-coating reflection from the similar colored coating to the incident beam.[22] For another red coating (coating 20), the coating-core interface is not visible

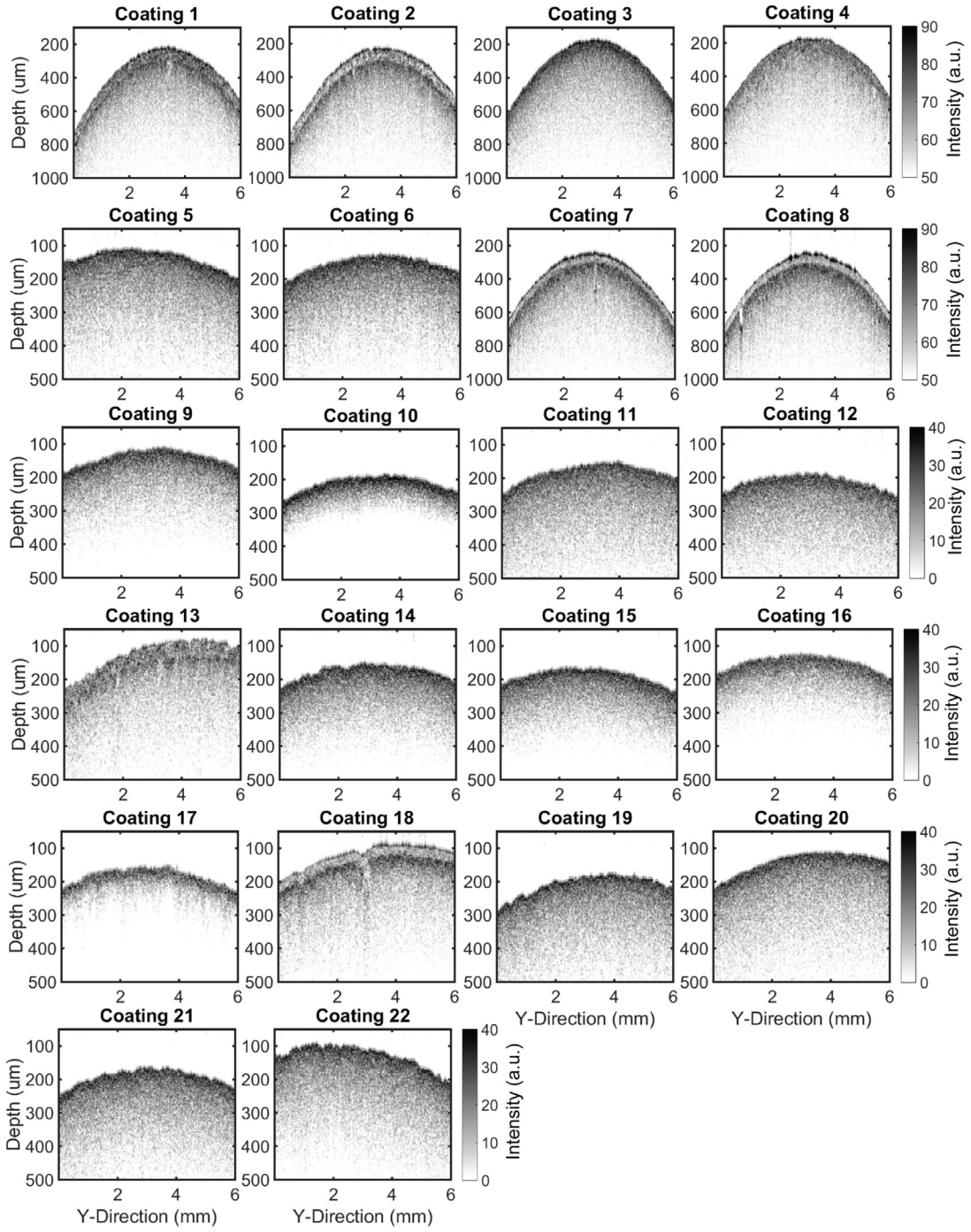

Figure 2. B-scans of the coated tablets where the air-coating interface can be observed and the coating-core interface is only visible for only coatings 1, 2, 7, 8, 13, and 18.

due to the titanium dioxide used in a comparatively thicker coating (10% weight gain). Finally, it is interesting to note that where the coating contains only talc and dye in the colorant as in the case of coating 13, the coating-core interface is marginally visible in the OCT measurements.

Conclusion

With the emergence of OCT for the non-destructive evaluation of pharmaceutical coatings, it is important to know the limitations of the technique. We have presented OCT measurements for a range of pigments and formulations based on a popular immediate release coating platform used in the pharmaceutical industry today. Our findings show that coating transparency for OCT measurement ultimately depends on the pigment type, coating formulation, and the tablet core as well as the coating process itself. Our findings further show that where the coating material contains titanium dioxide, either alone or together with other pigments, OCT measurement becomes adversely affected by scattering resulting in a blurred coating-core interface that makes coating thickness quantification impossible. For coatings without titanium dioxide, coating transparency is not always guaranteed. In order to precisely explain our measurements, mechanistic modeling could be applied. We therefore envision that OCT might be best suited for process

Table 2
Coating Compositions of the Coating Aliases With the Highlighted Rows Corresponding to OCT Transparency

Coating	Nominal Weight Gain	Measured Weight Gain (%)	Estimated Coating Thickness (μm)	Polymer	Plasticizer	Colorants		Auxiliary
						Pigment	Dye	
Coating 1	3%	5.1 ± 1.1	40 ± 3	HPMC	PEG			
Coating 2	3%	5.5 ± 1.1	54 ± 5	HPMC HPC				
Coating 3	3%	6.2 ± 1.1	46 ± 4	HPMC	PEG			Lactose
Coating 4	3%	6.0 ± 1.1	50 ± 3	HPMC	Propylene glycol			Polydextrose
Coating 5	3%	3.4 ± 1.1	47 ± 9	HPMC		Red iron oxide Yellow iron oxide Titanium dioxide Talc		
Coating 6	3%	2.1 ± 1.2	27 ± 13	HPMC	PEG	Yellow iron oxide Titanium dioxide		
Coating 7	3%	5.1 ± 1.2	37 ± 4	PVA	PEG	Talc		
Coating 8	3%	5.7 ± 1.1	41 ± 3	Sodium CMC		Tapioca dextrin		Lecithin Sodium citrate Dextrose
Coating 9	3%	3.6 ± 1.1	59 ± 10	HPMC	PEG	Yellow iron oxide		
Coating 10	3%	3.2 ± 1.4	50 ± 18	HPMC	PEG Triacetin	Yellow iron oxide Black oxide Titanium dioxide		Lactose
Coating 11	3%	3.4 ± 1.0	53 ± 9	HPMC	PEG	Titanium dioxide	Blue	Capmul
Coating 12	3%	3.5 ± 1.1	55 ± 11	HPMC	PEG	Titanium dioxide Talc	Blue	
Coating 13	3%	3.1 ± 1.1	52 ± 10	PVA	PEG	Talc	Blue	
Coating 14	3%	3.4 ± 1.3	47 ± 12	PVA	PEG	Black oxide Carmine Titanium dioxide Talc	Blue	Lecithin
Coating 15	4%	4.3 ± 1.1	52 ± 12	PVA		Titanium dioxide Talc	Cu-chlorophyllin	SLS
Coating 16	4%	5.0 ± 1.1	59 ± 10	HPMC HPC		Titanium dioxide Talc	Cu-chlorophyllin	
Coating 17	3%	3.3 ± 1.2	60 ± 14	PVA	PEG	Riboflavine Spirilina Veg carbon black Titanium dioxide Talc		
Coating 18	3%	2.2 ± 1.1	28 ± 12	PVA	PEG	Yellow iron oxide Carmine Talc		Polysorbate
Coating 19	4%	6.4 ± 1.4	70 ± 15	PVA Eudragit	PEG	Yellow iron oxide Titanium dioxide Talc	Blue Yellow	
Coating 20	10%	9.9 ± 1.6	105 ± 13	Eudragit		Carmine Titanium dioxide Talc		Poloxamer SLS Sodium bicarbonate Calcium silicate
Coating 21	3%	3.4 ± 1.1	48 ± 10	PVA	PEG	Titanium dioxide Talc	Blue Yellow	Lecithin
Coating 22	3%	3.8 ± 1.2	54 ± 12	HPMC	Propylene glycol	Titanium dioxide	Blue	

The weight and tablet thickness were measured of 6 tablets per batch. The coating thickness and weight gain were calculated from the average weight and tablet thickness measurements of each batch and the tablet core. The standard deviation was calculated by applying the error propagation law.
HPMC, hydroxypropyl methylcellulose; PEG, polyethylene glycol; PVA, poly(vinyl alcohol); CMC, carboxymethyl cellulose; SLS, sodium lauryl sulfate; HPC, hydroxypropyl cellulose.

analytical technology applications of functional polymeric coatings, and in particular for multiparticulates where high pigmentations can be avoided.[10-15,23] For coatings on tablets where pigments cannot be avoided, TPI is a proven alternative for coating thickness greater than 30-40 μm.[6,24]

Acknowledgments

The authors would like to acknowledge the financial support from UK EPSRC Research Grant EP/L019787/1 and EP/L019922/1. The authors acknowledge Colorcon Ltd. (Dartford, UK) for providing the materials used in this study. H.L. also acknowledges travel support from Joy Welch Educational Charitable Trust.

References

1. Suzzi D, Toschkoff G, Radl S, et al. DEM simulation of continuous tablet coating: effects of tablet shape and fill level on inter-tablet coating variability. *Chem Eng Sci*. 2012;69:107-121.
2. Romero-Torres S, Pérez-Ramos JD, Morris KR, Grant ER. Raman spectroscopic measurement of tablet-to-tablet coating variability. *J Pharm Biomed Anal*. 2005;38(2):270-274.
3. McGoverin CM, Rades T, Gordon KC. Recent pharmaceutical applications of Raman and terahertz spectroscopies. *J Pharm Sci*. 2008;97:4598-4621.
4. Ricci C, Nyadong L, Fernandez FM, Newton PN, Kazarian SG. Combined Fourier-transform infrared imaging and desorption electrospray-ionization linear ion-trap mass spectrometry for analysis of counterfeit antimalarial tablets. *Anal Bioanal Chem*. 2007;387:551-559.
5. Djemai A, Sinka IC. NMR imaging of density distributions in tablets. *Int J Pharm*. 2006;319:55-62.
6. Zeitler JA, Shen Y, Baker C, Taday PF, Pepper M, Rades T. Analysis of coating structures and interfaces in solid oral dosage forms by three dimensional terahertz pulsed imaging. *J Pharm Sci*. 2007;96:330-340.
7. Zeitler JA, Gladden LF. In-vitro tomography and non-destructive imaging at depth of pharmaceutical solid dosage forms. *Eur J Pharm Biopharm*. 2009;71:2-22.
8. Lin H, May RK, Evans MJ, et al. Impact of processing conditions on inter-tablet coating thickness variations measured by terahertz in-line sensing. *J Pharm Sci*. 2015;104(8):2513-2522.
9. Mauritz JM, Morrisby RS, Hutton RS, Legge CH, Kaminski CF. Imaging pharmaceutical tablets with optical coherence tomography. *J Pharm Sci*. 2010;99:385-391.
10. Zhong S, Shen Y-C, Ho L, et al. Non-destructive quantification of pharmaceutical tablet coatings using terahertz pulsed imaging and optical coherence tomography. *Opt Lasers Eng*. 2011;49:361-365.
11. Koller DM, Hannesschlager G, Leitner M, Khinast JG. Non-destructive analysis of tablet coatings with optical coherence tomography. *Eur J Pharm Sci*. 2011;44:142-148.
12. Li C, Zeitler JA, Dong Y, Shen YC. Non-destructive evaluation of polymer coating structures on pharmaceutical pellets using full-field optical coherence tomography. *J Pharm Sci*. 2014;103:161-166.
13. Markl D, Zettl M, Hannesschläger G, et al. Calibration-free in-line monitoring of pellet coating processes via optical coherence tomography. *Chem Eng Sci*. 2015;125:200-208.
14. Markl D, Hannesschläger G, Sacher S, Leitner M, Khinast JG. Optical coherence tomography as a novel tool for in-line monitoring of a pharmaceutical film-coating process. *Eur J Pharm Sci*. 2014;55:58-67.
15. Markl D, Hannesschläger G, Sacher S, et al. In-line monitoring of a pharmaceutical pan coating process by optical coherence tomography. *J Pharm Sci*. 2015;104(8):2531-2540.
16. Lin H, Dong Y, Shen YC, Zeitler JA. Quantifying pharmaceutical film coating with optical coherence tomography and terahertz pulsed imaging: an evaluation. *J Pharm Sci*. 2015;104(10):3377-3385.
17. Markl D, Hannesschläger G, Sacher S, Leitner M, Khinast JG, Buchsbaum A. Automated pharmaceutical tablet coating layer evaluation of optical coherence tomography images. *Meas Sci Technol*. 2015;26:035701.
18. Ruotsalainen M, Heinämäki J, Guo H, Laitinen N, Yliruusi J. A novel technique for imaging film coating defects in the film-core interface and surface of coated tablets. *Eur J Pharm Sci*. 2003;56(3):381-388.
19. Pourkavoos N, Peck GE. The effect of swelling characteristics of super-disintegrants on the aqueous coating solution penetration into the tablet matrix during the film coating process. *Pharm Res*. 1993;10(9):1363-1371.
20. Song J, Qin J, Qu J, et al. The effects of particle size distribution on the optical properties of titanium dioxide rutile pigments and their applications in cool non-white coatings. *Sol Mater Sol Cells*. 2014;130:42-50.
21. Levinson R, Berdahl P, Akbari H. Solar spectral optical properties of pigments—part II: survey of common colorants. *Sol Energy Mater Sol Cells*. 2005;89(4):351-389.
22. Levinson R, Berdahl P, Akbari H. Solar spectral optical properties of pigments—part I: model for deriving scattering and absorption coefficients from transmittance and reflectance measurements. *Sol Mater Sol Cells*. 2005;89(4):319-349.
23. Lin H, Dong Y, Markl D, et al. Measurement of the inter-tablet coating uniformity of a pharmaceutical pan coating process with combined terahertz and optical coherence tomography in-line sensing. *J Pharm Sci*. 2017;106(4):1075-1084.
24. May RK, Evans MJ, Zhong S, et al. Terahertz in-line sensor for direct coating thickness measurement of individual tablets during film coating in real-time. *J Pharm Sci*. 2011;100(4):1535-1544.